



(±)-Peniorthoesters A and B, Two Pairs of Novel Spiro-Orthoester en-antiomers With an Unusual 1,4,6-Trioxaspi-ro[4.5]decane-7-One Unit From *Penicillium minioluteum*

Xiaorui Liu[†], Chunmei Chen[†], Yinyu Zheng, Mi Zhang, Qingyi Tong, Junjun Liu, Qun Zhou, Jianping Wang, Zengwei Luo, Hucheng Zhu* and Yonghui Zhang*

Hubei Key Laboratory of Natural Medicinal Chemistry and Resource Evaluation, School of Pharmacy, Tongji Medical College, Huazhong University of Science and Technology, Wuhan, China

OPEN ACCESS

Edited by:

Bin-Gui Wang,
Institute of Oceanology (CAS), China

Reviewed by:

Dipesh Dhakal,
Sun Moon University, South Korea
Christophe Salome,
SpiroChem AG, Switzerland

*Correspondence:

Hucheng Zhu
zhuhucheng@hust.edu.cn
Yonghui Zhang
zhangyh@mails.tjmu.edu.cn

[†]These authors have contributed
equally to this work

Specialty section:

This article was submitted to
Medicinal and Pharmaceutical
Chemistry,
a section of the journal
Frontiers in Chemistry

Received: 02 August 2018

Accepted: 26 November 2018

Published: 07 December 2018

Citation:

Liu X, Chen C, Zheng Y, Zhang M,
Tong Q, Liu J, Zhou Q, Wang J,
Luo Z, Zhu H and Zhang Y (2018)
(±)-Peniorthoesters A and B, Two
Pairs of Novel Spiro-Orthoester
en-antiomers With an Unusual
1,4,6-Trioxaspi-ro[4.5]decane-7-One
Unit From *Penicillium minioluteum*.
Front. Chem. 6:605.
doi: 10.3389/fchem.2018.00605

(±)-Peniorthoesters A and B (±1 and ±2), two pairs of unprecedented spiro-orthoester enantiomers with a 1,4,6-trioxaspiro[4.5]decane-7-one unit, were obtained from *Penicillium minioluteum*. Their structures were determined by spectroscopic methods, X-ray diffraction analyses, and ECD calculations. (±)-Peniorthoesters A and B are the first examples of spiro-orthoester enantiomers, and they represent the first spiro-orthoesters originating from fungi. All compounds showed potential inhibitory activities comparable to dexamethasone against NO production with IC₅₀ values ranging from 14.2 to 34.5 μM.

Keywords: peniorthoesters, *Penicillium minioluteum*, spiro-orthoester, enantiomers, NO production inhibition activity

INTRODUCTION

Orthoesters, a special functional group characterized by three alkoxy groups attached to a single carbon atom, are unusual structural subunits in natural products (Liao et al., 2009). Natural occurring orthoesters include several major types, such as daphnane diterpenoid orthoesters (He et al., 2002), limonoid orthoesters (Roy and Saraf, 2006), steroid orthoesters (Steyn and van Heerden, 1998), and coumarinoid orthoesters (Santana et al., 2004). In our previous study on the plant *Wikstroemia chamaedaphne*, three new daphnane type diterpenoids with orthoester group were isolated (Guo et al., 2015). A literature investigation revealed that most of these orthoesters originate from plants, and only a few originate from fungi, such as novofumigatonin, a meroterpenoid orthoester from *Aspergillus novofumigatus* (Rank et al., 2008). As a special class of natural products, orthoesters have attracted great attention due to their diverse structures and biological properties (Liao et al., 2009; Bourjot et al., 2014; Li et al., 2015; Liu et al., 2017).

Fungi have historically played an important role in drug discovery. The genus *Penicillium* has been shown to be a rich source of structurally unique and biologically active secondary metabolites (Meng et al., 2016; Sun et al., 2016; Luo et al., 2017) and many metabolites from *Penicillium* are clinically used drugs with penicillin as a representative compound. Previous studies on the secondary metabolites of *Penicillium minioluteum* have resulted in the identification of scores of bioactive metabolites, including isomeric furanones with cytotoxic activities against HeLa cell lines (Tang et al., 2015), sesquiterpene-conjugated amino acids with cytotoxic activities against HepG2 cells (Ngokpol et al., 2015), and hybrid polyketide-terpenoids (Iida et al., 2008). This fungus

was also used to produce clovane derivatives, which are the raw materials for the synthesis of rumphellclovane A (Gontijo de Souza et al., 2012), and an enzyme from this fungus was used in the bioconversion (Kmieciak and Zymanczyk-Duda, 2017). During our ongoing search for structurally unique and biologically interesting constituents from fungi (Zhu et al., 2015; Chen et al., 2017; Zhou et al., 2017), *P. minioluteum*, obtained from China General Micro-biological Culture Collection Center (CGMCC), was phytochemically investigated, and two pairs of new orthoesters (**Figure 1**, compounds ±**1** and ±**2**) were isolated along with their biosynthetic intermediate, sclerotinin A (**3**) (Xiao et al., 2009). The structures and absolute configurations of (±)-**1** and (±)-**2** were determined by a combination of spectroscopic methods, X-ray diffraction analyses, and ECD calculations. (±)-Peniorthoesters A (±**1**) and B (±**2**) are the first examples of spiro-orthoester enantiomers and represent the first spiro-orthoesters originating from fungi.

MATERIALS AND METHODS

General Experimental Procedures

Optical rotations were determined in acetonitrile and dichloromethane on a PerkinElmer 341 polarimeter. UV spectra were obtained on Varian Cary 50 spectrometer. ECD spectra were obtained with a JASCO J-810 spectrometer. IR spectra were acquired on a Bruker Vertex 70 instrument. NMR spectra were recorded on Bruker AM-400 spectrometers, and the ^1H and ^{13}C NMR chemical shifts were referenced to the solvent or solvent impurity peaks for CD_3Cl at δ_{H} 7.26 and δ_{C} 77.20. HRESIMS data were acquired in the positive-ion mode on a Thermo Fisher LC-LTQ-Orbitrap XL spectrometer. The crystallographic experiments were performed on a Bruker APEX DUO diffractometer equipped with graphite-monochromated $\text{Cu K}\alpha$ radiation ($\lambda = 1.54178 \text{ \AA}$). Semi-preparative HPLC was carried out on an instrument consisting of an Agilent 1,220 controller, an Agilent 1,220 pump, an Agilent UV detector, with a reversed-phased C18 column ($5 \mu\text{m}$, $10 \times 250 \text{ mm}$, Welch Ultimate XB-C18), an Ultimate SiO_2 column ($5 \mu\text{m}$, $10 \times 250 \text{ mm}$, Welch Materials, Inc.), and a Chiralpak IC column ($5 \mu\text{m}$, $4.6 \times 250 \text{ mm}$, Daicel Chiral Technologies Co., Ltd., China). Chromatography columns (CC) were performed on silica gel (200–300 mesh; Qingdao Marine Chemical, Inc., Qingdao, China), Sephadex LH-20 ($40\text{--}70 \mu\text{m}$, Amersham Pharmacia Biotech AB, Uppsala, Sweden), and ODS ($50 \mu\text{m}$, Merck, Germany). Thin-layer chromatographies (TLC) was performed with RP-C₁₈ F₂₅₄ plates (Merck, Germany) and silica gel 60 F₂₅₄ (Yantai Chemical Industry Research Institute).

Fungal Material and Fermentation

The strain in this work was bought from China General Micro-biological Culture Collection Center (CGMCC). A voucher Specimen was preserved in the herbarium of Huazhong University of Science and Technology, China. The fungal strain was cultured on potato dextrose agar (PDA) at 28°C for 8 days to prepare the seed culture. Then the strain was inoculated into 200 Erlenmeyer flasks (1 L each) which had previously been sterilized by autoclaving. Each flask contained 250 g rice and

200 mL distilled water. The flasks were incubated at 20°C for 26 days.

Extraction and Isolation

The fermented rice substrate was extracted six times in 95% aqueous EtOH at room temperature. The 95% aqueous EtOH extracts were concentrated under vacuum to afford a residue (1.5 kg). The residue was suspended in H_2O and successively partitioned with petroleum ether and EtOAc. The EtOAc partition fraction (630.0 g) was subjected to a silica gel chromatograph column (CC) using petroleum ether–EtOAc and EtOAc–MeOH gradient elution to give five fractions. Fraction 2 (20.0 g) was chromatographed on C18 reversed phase (RP-18) silica gel CC (gradient elution of MeOH– H_2O , 20:80–100:0) to give seven subfractions, named Fr. 2A–2G. Fr.2F was successively separated via Sephadex LH-20 CC (CH_2Cl_2 –MeOH, 1:1) and further purified by RP-C₁₈ HPLC to afford compounds **1** and **2** (MeCN– H_2O , 45:55, 3.5 ml/min, **1** at t_{R} 53.2 min, 6.0 mg; **2** at t_{R} 56.7 min, 5.1 mg). Subsequently, the separation of **1** by chiral HPLC using a Daicel IC column eluting with isopropanol–*n*-hexane (5:95) afforded (+)-**1** (t_{R} 28.0 min, 2.1 mg) and (–)-**1** (t_{R} 30.1 min, 2.0 mg). The enantiomers (+)-**2** (t_{R} 8.2 min, 1.6 mg) and (–)-**2** (t_{R} 11.1 min, 2.7 mg) were also obtained by chiral HPLC using a Daicel IC column eluting with isopropanol–*n*-hexane (10:90).

Compounds (±)-**1**: white powder; $[\alpha]_{\text{D}}^{25} \pm 0$ (c 0.4, MeCN); UV (MeCN) λ_{max} (log ϵ) 216 (4.50), 259 (4.23), 329 (4.04) nm; IR (KBr) ν_{max} 3,435, 2,982, 2,936, 1,661, 1,612, 1,456, 1,420, 1,383, 1,341, 921, 883, 809, 753 cm^{-1} ; ^1H NMR (CDCl_3 , 400 MHz) and ^{13}C NMR (CDCl_3 , 100 MHz) data, see **Table 1**; HRESIMS m/z 307.1538 $[\text{M} + \text{H}]^+$ (calcd for $\text{C}_{17}\text{H}_{23}\text{O}_5$, 307.1545).

(+)-**1**: white amorphous powder; $[\alpha]_{\text{D}}^{25} +37$ (c 0.1, CH_2Cl_2); ECD (MeCN) 229 ($\Delta\epsilon +1.63$), 254 ($\Delta\epsilon +4.75$), 325 ($\Delta\epsilon -0.99$) nm.

(–)-**1**: white amorphous powder; $[\alpha]_{\text{D}}^{25} -36$ (c 0.1, CH_2Cl_2); ECD (MeCN) 229 ($\Delta\epsilon -1.66$), 254 ($\Delta\epsilon -4.34$), 325 ($\Delta\epsilon +1.23$) nm.

Compounds (±)-**2**: white powder; $[\alpha]_{\text{D}}^{25} \pm 0$ (c 0.3, MeCN); UV (MeCN) λ_{max} (log ϵ) 216 (4.60), 259 (3.99), 329 (3.71) nm; IR (KBr) ν_{max} 3,435, 2,980, 2,932, 1,669, 1,612, 1,456, 1,421, 1,379, 1,339, 920, 881, 810, 763 cm^{-1} ; ^1H NMR (CDCl_3 , 400 MHz) and ^{13}C NMR (CDCl_3 , 100MHz) data, see **Table 1**; HRESIMS m/z 307.1534 $[\text{M} + \text{H}]^+$ (calcd for $\text{C}_{17}\text{H}_{23}\text{O}_5$, 307.1545).

(+)-**2**: white amorphous powder; $[\alpha]_{\text{D}}^{25} +30$ (c 0.1, CH_2Cl_2); ECD (MeCN) 224 ($\Delta\epsilon +2.37$), 258 ($\Delta\epsilon +4.64$), 319 ($\Delta\epsilon -0.84$) nm.

(–)-**2**: white amorphous powder; $[\alpha]_{\text{D}}^{25} -30$ (c 0.1, CH_2Cl_2); ECD (MeCN) 224 ($\Delta\epsilon -2.42$), 258 ($\Delta\epsilon -6.58$), 319 ($\Delta\epsilon +1.60$) nm.

Computational Details

The crystal structure of 9*R*,10*S*,11*S*-**1**, and 9*R*,10*R*,11*R*-**2** were optimized at the B3LYP/6-31G(d) level in acetonitrile with the IEFPCM solvation model using Gaussian 09 program. The harmonic vibrational frequencies were calculated to confirm the stability of the optimized structure. The electronic

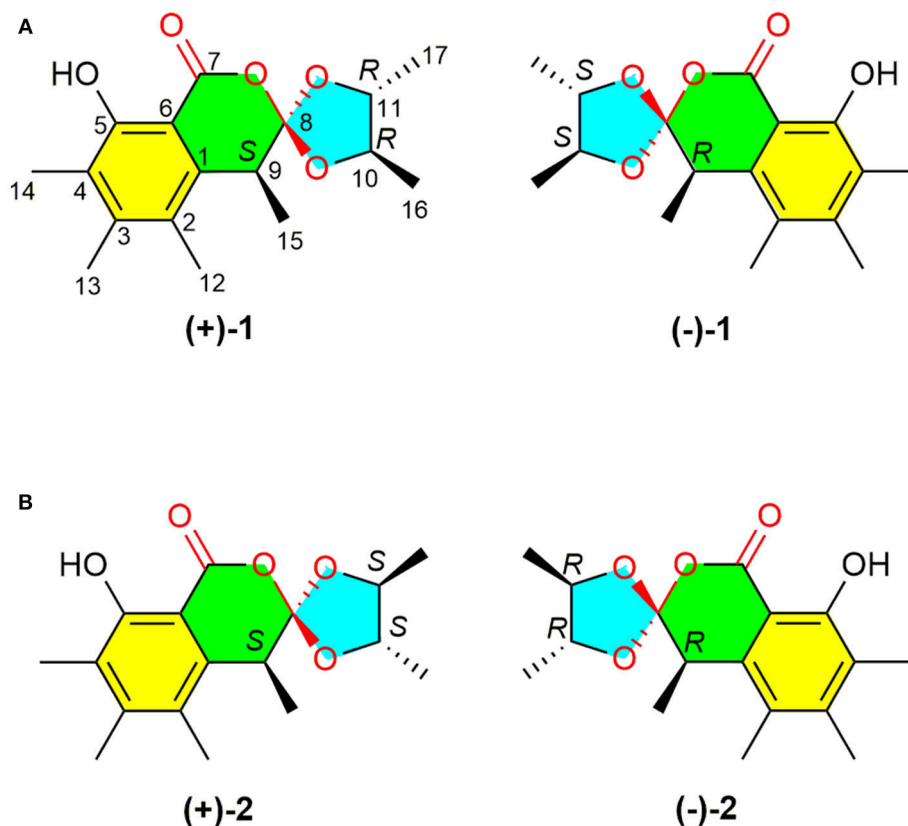


FIGURE 1 | Structures of (±)-peniorthoesters A (±1) and B (±2).

circular dichroism (ECD) spectrum were calculated using the TDDFT methodology at the LC-wPBE/6-311++G(d,p) level with acetonitrile as solvent by the IEFPCM solvation model implemented in Gaussian 09 program. The ECD spectra was simulated using a Gaussian function with a bandwidth σ of 0.3 eV. The UV correction was applied to generate the final spectra (Zhu, 2015).

Single-Crystal X-ray Diffraction Analysis and Crystallographic Data

Crystallographic data of compound **1** (CCDC 1840165): $C_{17}H_{22}O_5$, $M = 306.34$, monoclinic, $T = 297(2)$ K, $\lambda = 1.54178$ Å, colorless platelet (crystallized from distilled water at room temperature), size $0.12 \times 0.10 \times 0.10$ mm³, $a = 11.7937(4)$ Å, $b = 32.5593(12)$ Å, $c = 8.1659(3)$ Å, $\alpha = 90.00^\circ$, $\beta = 91.95(2)^\circ$, $\gamma = 90.00^\circ$, $V = 3,133.84(19)$ Å³, space group $P21/c$, $Z = 8$, $D_c = 1.299$ g/cm³, $\mu(\text{CuK}\alpha) = 0.782$ mm⁻¹, $F_{(000)} = 1312$, 48082 reflections and 5,729 independent reflections ($R_{\text{int}} = 0.0528$) were collected in the θ range of $2.71^\circ \leq \theta \leq 69.99^\circ$ with index ranges of $h(-14/14)$, $k(-39/39)$, $l(-9/9)$, completeness $\theta_{\text{max}} = 98\%$, data/restraints/parameters 5,729/0/412. Largest difference peak and hole = 0.257 and -0.184 e Å⁻³. The final R_1 values were 0.0489 ($I > 2\sigma(I)$). The final $wR(F^2)$ values were 0.1364 ($I >$

$2\sigma(I)$). The final R_1 values were 0.0521 (all data). The final $wR(F^2)$ values were 0.1381 (all data). The goodness of fit on F^2 was 1.045.

Crystallographic data of compound **2** (CCDC 1840166): $C_{17}H_{22}O_5$, $M = 306.34$, monoclinic, $T = 297(2)$ K, $\lambda = 1.54178$ Å, colorless platelet (crystallized from distilled water at room temperature), size $0.12 \times 0.10 \times 0.10$ mm³, $a = 7.4709(2)$ Å, $b = 8.9377(12)$ Å, $c = 13.5720(3)$ Å, $\alpha = 92.43^\circ$, $\beta = 100.25(2)^\circ$, $\gamma = 113.76^\circ$, $V = 809.60(19)$ Å³, space group $P-1$, $Z = 2$, $D_c = 1.257$ g/cm³, $\mu(\text{CuK}\alpha) = 0.757$ mm⁻¹, $F_{(000)} = 328$, 14,855 reflections and 2,814 independent reflections ($R_{\text{int}} = 0.0374$) were collected in the θ range of $5.45^\circ \leq \theta \leq 70.86^\circ$ with index ranges of $h(-8/7)$, $k(-10/10)$, $l(-16/16)$, completeness $\theta_{\text{max}} = 95\%$, data/restraints/parameters 2,814/0/207. Largest difference peak and hole = 0.232 and -0.241 e Å⁻³. The final R_1 values were 0.0588 ($I > 2\sigma(I)$). The final $wR(F^2)$ values were 0.1750 ($I > 2\sigma(I)$). The final R_1 values were 0.0647 (all data). The final $wR(F^2)$ values were 0.1855 (all data). The goodness of fit on F^2 was 1.076.

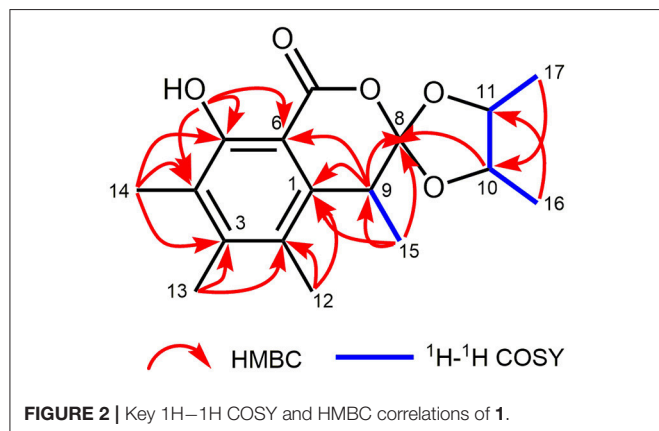
Determination of No Production

RAW 264.7 cells were obtained from the Boster Biological Technology Co., Ltd (Wuhan, China) and maintained in DMEM containing 10% heat-inactivated fetal bovine serum (FBS) (Gibco BRL Co, Grand Island, NY, United States) at 37°C in humidified incubator containing 5% CO₂. All tested compounds were dissolved in DMSO (the final concentration of DMSO was

TABLE 1 | ^1H and ^{13}C NMR Spectroscopic Data for **1** and **2** (in CDCl_3).

No.	1			2		
	δ_{C}	type	δ_{H} (mult., J in Hz)	δ_{C}	type	δ_{H} (mult., J in Hz)
1	137.8	C		137.6	C	
2	123.5	C		123.6	C	
3	145.7	C		145.7	C	
4	123.7	C		123.8	C	
5	158.8	C		158.7	C	
6	103.5	C		103.7	C	
7	170.3	C		170.2	C	
8	124.0	C		124.0	C	
9	38.4	CH	3.31 q (7.1)	38.5	CH	3.33 q (7.0)
10	81.7 ^a	CH	3.91 dq (8.5, 6.1) ^a	81.1 ^a	CH	3.84 dq (8.1, 6.2) ^a
11	79.3 ^a	CH	4.18 dq (8.5, 6.1) ^a	79.8 ^a	CH	4.36 dq (8.1, 6.2) ^a
12	14.7	CH ₃	2.17 s	14.6	CH ₃	2.17 s
13	17.5	CH ₃	2.25 s	17.4	CH ₃	2.24 s
14	11.9	CH ₃	2.20 s	11.9	CH ₃	2.20 s
15	16.9	CH ₃	1.30 d (7.1)	17.2	CH ₃	1.30 brd (6.3)
16	16.7 ^a	CH ₃	1.47 d (6.1) ^a	16.7 ^a	CH ₃	1.30 brd (6.1) ^a
17	18.4 ^a	CH ₃	1.25 d (6.1) ^a	18.6 ^a	CH ₃	1.39 d (6.1) ^a
HO-5			11.41 s			11.41 s

^aInterchangeable assignments between the two CHCH_3 groups.



<0.25% in assay). RAW 264.7 cells were seeded into 48-well plates (1×10^5 cells/well) for 24 h and then pretreated with different concentrations (1–40 μM) of test compounds. After being incubated for 3 h, the cells were stimulated with 100 ng/ml LPS (final concentration) for another 24 h. Dexamethasone was used as the positive control in the experiment. NO content in the supernatant was measured using Griess reagent. The absorbance at 540 nm was measured on a microplate reader. All the experiments were performed in three independent replicates.

Cytotoxic Activity

Cell lines were cultured in RPMI-1640 or DMEM medium (HyClone, USA), supplemented with 10% fetal bovine serum

(HyClone, USA) at 37°C in a humidified atmosphere with 5% CO_2 . For cell viability assay, cells were plated into 96-well plates in 50 μl of medium and then compounds were serially diluted in medium and delivered to the cells as $2 \times$ solutions in 50 μl of medium. After 48 h, cell viability was detected by a CCK-8 Kit (Dojindo, Japan) according to the instruction. Growth relative to untreated cells was calculated (positive control, anticancer drug VP16), and this data was used for the dose-response curve, the IC_{50} (50% inhibiting concentration) of compounds to each cell lines were calculated by SPSS.

RESULTS AND DISCUSSIONS

Compound **1** was isolated as a white powder. Its UV spectrum exhibited absorption maxima at 216 and 260 nm. Its IR spectrum indicated the presence of an OH functionality ($3,435\text{ cm}^{-1}$), a conjugated carbonyl group ($1,661\text{ cm}^{-1}$), and an aromatic ring ($1,612$ and $1,456\text{ cm}^{-1}$). The molecular formula of **1** was determined to be $\text{C}_{17}\text{H}_{22}\text{O}_5$ by HRESIMS with an $[\text{M} + \text{H}]^+$ ion peak at m/z 307.1538 (calcd for $\text{C}_{17}\text{H}_{23}\text{O}_5$, 307.1545), implying seven degrees of unsaturation. The ^1H NMR spectroscopic data of **1** (Table 1) revealed the presence of two oxygenated methines [δ_{H} 4.18 (1H, dq, $J = 8.5, 6.1$ Hz, H-11) and 3.91 (1H, dq, $J = 8.5, 6.1$ Hz, H-10)], one sp^3 methine [δ_{H} 3.31, 1H, q, $J = 7.1$ Hz, H-9], and six methyl groups [δ_{H} 1.47 (d, $J = 6.1$ Hz, H₃-16), 1.30 (d, $J = 7.1$ Hz, H₃-15), 1.25 (d, $J = 6.1$ Hz, H₃-17), 2.17 (s, H₃-12), 2.20 (s, H₃-14), and 2.25 (s, H₃-13)]. The ^{13}C NMR spectrum of **1** exhibited signals assignable to a conjugated carbonyl (δ_{C} 170.3), a hexa-substituted benzene ring [δ_{C} 158.8, 145.7, 137.8,

123.7, 123.5, and 103.5], one oxygenated quaternary carbon (δ_C 124.0), six methyl groups and three methines (including two oxygenated ones). The above analyses confirmed the presence of an ester carbonyl group and a hexa-substituted benzene ring, which account for five degrees of unsaturation, indicating the presence of two additional rings. With the aid of the HSQC spectrum, all protons were unambiguously assigned to their respective carbons.

The planar structure of **1** was elucidated on the basis of ^1H - ^1H COSY and HMBC experiments (Figure 2). The HMBC spectrum of **1** displayed correlations from H₃-14 to C-3, C-4, and C-5; from H₃-13 to C-2, C-3, and C-4; from H₃-12 to C-1, C-2, and C-3; and from H-9 to C-1, and C-6, which together with the HMBC correlations from the OH to C-4, C-5, and C-6 constructed the hexa-substituted benzene ring. In addition, two spin systems of H₃-17/H-11/H-10/H₃-16 and H-9/H₃-15 were established from the ^1H - ^1H COSY spectrum. Therefore, the HMBC correlations from H-9 to C-1, C-6, and C-8 and from H₃-15 to C-1, C-8, and C-9 suggested the C-15/C-9/C-8 fragment was connected to the benzene ring via C-9. Moreover, the ester carbonyl (δ_C 170.3) was connected to C-6 based on the chemical shifts of C-6 (δ_C 103.5), C-1 (δ_C 137.8), and C-3 (δ_C 145.7). Combined with the chemical shifts of C-10 (δ_C 81.7) and C-11 (δ_C 79.3), the C-17/C-11/C-10/C-16 fragment was proposed to be a 2,3-butanediol unit, which should be linked with C-8 and form a 4,5-dimethyl-1,3-dioxolane moiety. Finally, a lactone ring was proposed between C-7 and C-8 to satisfy the above deduced tricyclic ring system as well as the chemical shift of C-8 (δ_C 124.0). This planar structure satisfied all of the correlations observed in the 2D NMR spectra and the chemical shifts in the 1D NMR spectra.

A NOESY experiment was performed on **1**, but no interactions useful for determining the relative configuration were observed. Unfortunately, the relative configuration of H-10 and H-11 could also not be determined from their coupling constants because they were located on a five-membered ring. To confidently assign the configuration of **1**, we tried to crystallize it so we could use X-ray single-crystal analysis. After a number of attempts, a high-quality single-crystal of **1** was finally obtained from a mixture of methyl alcohol and water. The X-ray crystallography data (CCDC 1840165) obtained with Cu K α radiation confirmed the structure of **1** (Figure 3). However, because it has a centrosymmetric monoclinic space group of chiral $P2_1/c$, indicating the crystal is racemic, the absolute configuration of **1** could not be determined. After analyses by using various types of chiral columns, the racemic nature of this solution was further confirmed by the presence of two peaks in the HPLC chromatogram acquired using a chiral Daicel IC column (Figure 4). Finally, compounds (+)-**1** and (-)-**1** were successfully obtained, and they showed specific rotations with opposite signs {(+)-**1**: $[\alpha]_D^{20} +37$ (c 0.1, CH₂Cl₂); (-)-**1**: $[\alpha]_D^{20} -36$ (c 0.1, CH₂Cl₂)}. In addition, the ECD spectra of (+)-**1** and (-)-**1** displayed similar signal intensities but mirror-image Cotton effects (Figure 5).

The absolute configurations of the two enantiomers of (±)-**1** were further determined by comparing their experimental ECD spectra with those predicted by time-dependent density

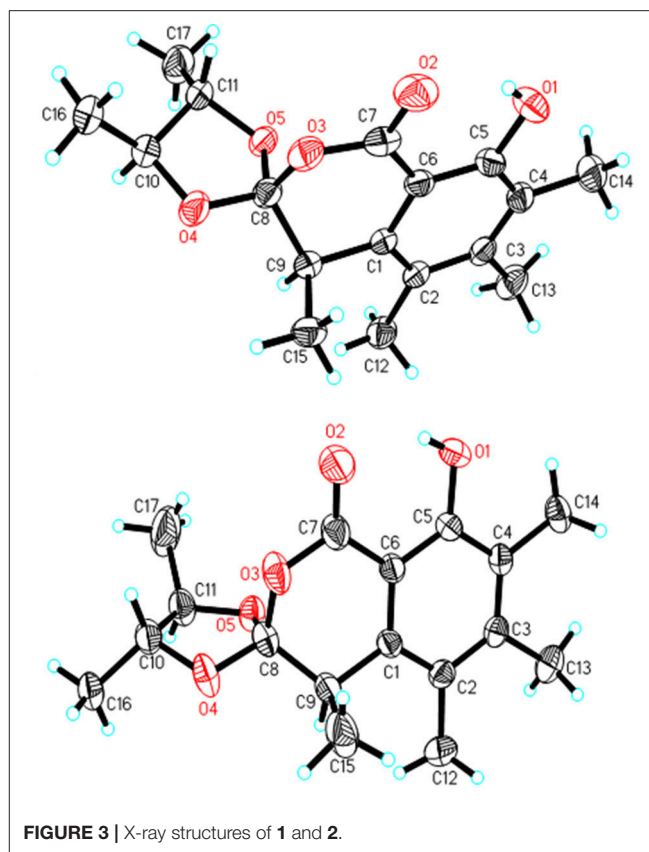


FIGURE 3 | X-ray structures of **1** and **2**.

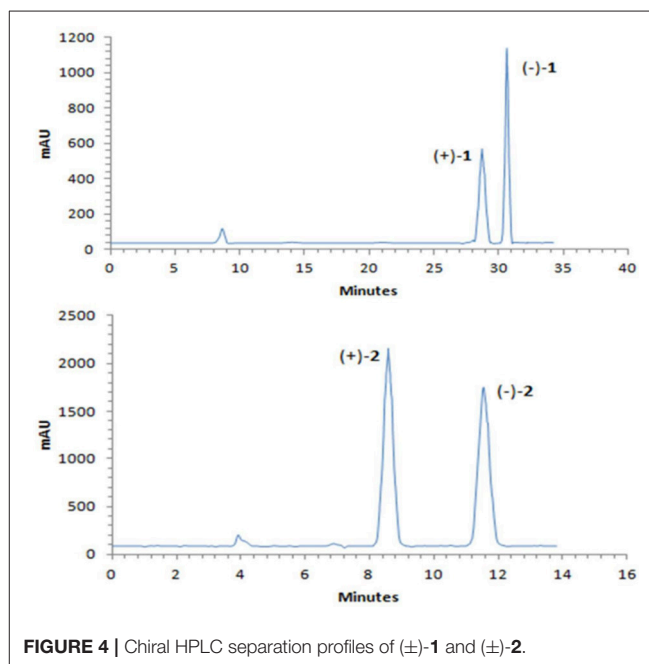


FIGURE 4 | Chiral HPLC separation profiles of (±)-**1** and (±)-**2**.

functional theory (TDDFT) calculations at the B3LYP/6-31G(d) level. As shown in Figure 5, the calculated ECD curve of 9R,10S,11S-**1** displayed good agreement with the experimental

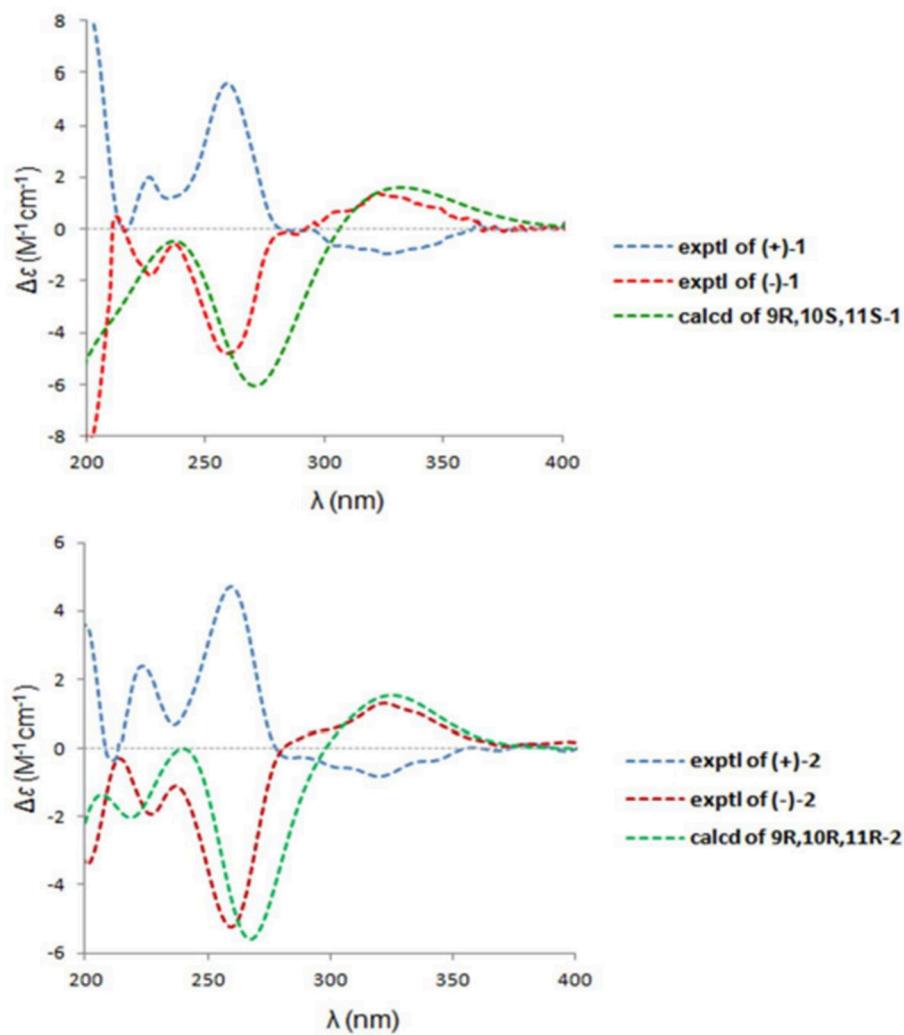


FIGURE 5 | The experimental ECD spectra of (±)-**1** and (±)-**2** and the calculated ECD curves.

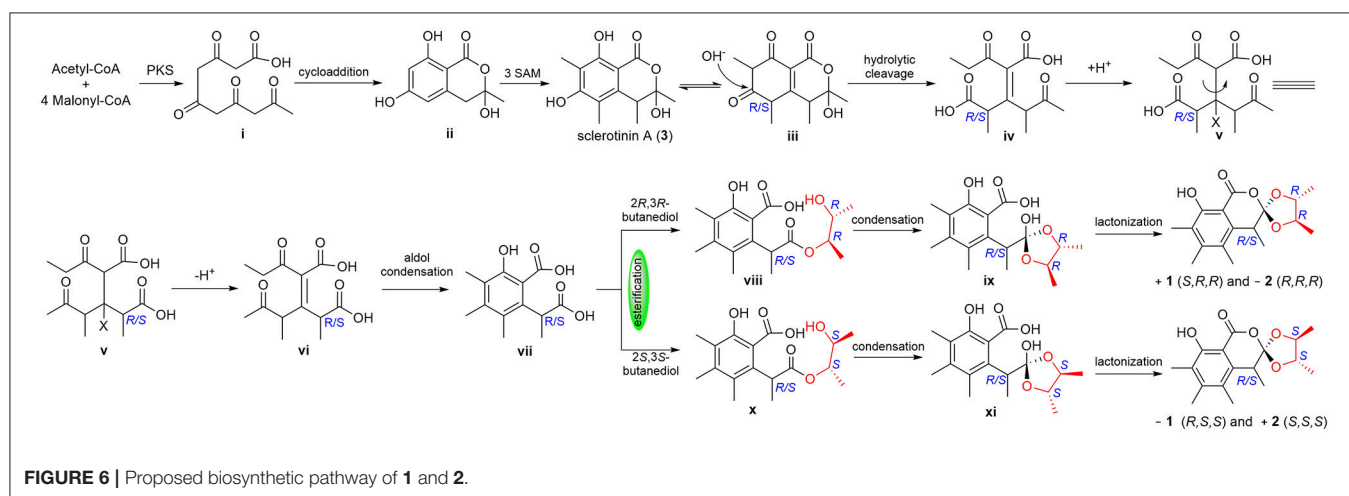


FIGURE 6 | Proposed biosynthetic pathway of **1** and **2**.

curve of (-)-**1**. Therefore, the absolute configurations of (+)-**1** and (-)-**1** were elucidated as 9*S*,10*R*,11*R* and 9*R*,10*S*,11*S*, respectively.

Compound **2**, obtained as a white powder, possesses the same molecular formula (C₁₇H₂₂O₅) as that of compound **1** based on its HRESIMS data with an [M + H]⁺ ion peak at *m/z* 307.1534 (calcd for C₁₇H₂₃O₅, 307.1545). A detailed comparison of its NMR spectroscopic data with those of **1** indicated that the main differences between **1** and **2** were tiny changes in the chemical shifts of C-10 and C-11 as well as their protons [δ_C 81.1 (C-10), 79.8 (C-11); δ_H 3.84 (1H, dq, *J* = 8.1, 6.2 Hz, H-10), 4.36 (1H, dq, *J* = 8.1, 6.2 Hz, H-11) in **2**; δ_C 81.7 (C-10), 79.3 (C-11); δ_H 3.91 (1H, dq, *J* = 8.5, 6.1 Hz, H-10), 4.18 (1H, dq, *J* = 8.5, 6.1 Hz, H-11) in **1**]. These findings, combined with the 2D NMR data, implied that **2** has the same planar structure as **1**, and it should be a stereoisomer of **1**. The planar structure of **2** was further confirmed by analyses of its ¹H-¹H COSY and HMBC spectra. Unfortunately, the NOESY experiment of **2** also did not show any NOESY correlations useful in for the elucidation of the relative configuration of compound **2**.

Similarly, after many attempts, we finally determined the relative configuration of compound **2** by X-ray crystallography analysis with Cu K α radiation (Figure 3, CCDC 1840166). This single-crystal is triclinic with space group of chiral P-1, also indicating it is racemic. Compound **2** was then separated into a pair of enantiomers by a method similar to what was used for compound **1** (Figure 4), and the enantiomers showed opposite optical rotations {(+)-**2**: [α]_D²⁰ +30 (c 0.1, CH₂Cl₂); (-)-**2**: [α]_D²⁰ -30 (c 0.1, CH₂Cl₂)} and mirror image ECD curves (Figure 5). The absolute configurations of the two enantiomers of **2** were further determined by ECD calculations. As shown in Figure 5, the calculated ECD curve of 9*R*,10*R*,11*R*-**2** closely resembled the experimental curve of (-)-**2**, and the absolute configurations of (+)-**2** and (-)-**2** were elucidated as 9*S*,10*S*,11*S* and 9*R*,10*R*,11*R*, respectively.

To the best of our knowledge, (±)-**1** and (±)-**2** are the first examples of spiro-orthoester enantiomers with an unusual 1,4,6-trioxaspiro[4.5]decane-7-one unit, and they represent the first spiro-orthoesters originating from fungi. The proposed biosynthetic pathway of **1** and **2** was outlined in Figure 6. First, the condensation of acetyl-CoA and four molecules of malonyl-CoA by a polyketide synthase formed **i**, which underwent cycloaddition and methylations to form precursor sclerotinin A (**3**). Then, sclerotinin A underwent isomerization and hydrolytic cleavage to afford **iv**, which further formed **vi** by a H⁺ mediated double bond isomerization. After that, intermediate **vii** was produced by an aldol condensation, which further generated the key intermediates **viii** and **x** via an esterification reaction with 2*R*,3*R*-butanediol and 2*S*,3*S*-butanediol (Ji et al., 2011), respectively. Finally, compounds (±)-**1** and (±)-**2** were formed via condensation and lactonization reactions.

Compounds (±)-**1** and (±)-**2** were tested for their inhibitory activities against NO production in lipopolysaccharide (LPS)-induced RAW264.7 cells. The results revealed that (+)-**1**, (-)-**1**, (+)-**2**, and (-)-**2** exhibited potential inhibitory activities

TABLE 2 | Inhibition of LPS-Induced NO Production.

Compound	IC ₅₀ (μM)
(+)- 1	34.5
(-)- 1	29.6
(+)- 2	23.5
(-)- 2	14.2
Dexamethasone	27.1

with IC₅₀ values of 34.5, 29.6, 23.5, and 15.2 μM, respectively (Table 2). Interestingly, for both pairs of enantiomers, the levorotatory compounds (-**1** and -**2**) showed better inhibitory effects than the dextrorotatory compounds (+**1** and +**2**). Moreover, both (+)-**2** and (-)-**2** showed better inhibitory effects than those of (+)-**1** and (-)-**1** as well as the positive control, dexamethasone. We also tested cytotoxicity of these compounds, but even at the concentration of 40 μM, none of them showed cytotoxicity activity.

CONCLUSION

In conclusion, two pairs of new spiro-orthoester enantiomers, (±)-peniorthoesters A and B (±**1** and ±**2**), were isolated from *P. minioluteum*. These compounds, characterized by an unexpected 1,4,6-trioxaspiro[4.5]decane-7-one unit, are the first examples of spiro-orthoester enantiomers, and they represent the first spiro-orthoesters originating from fungi. All of them showed potential inhibitory activities against NO production in activated macrophages with IC₅₀ values ranging from 14.2 to 34.5 μM, which are comparable to the positive control, dexamethasone. Their highly functionalized structures and promising biological activities will attract considerable attention from the pharmacological, synthetic, and biosynthetic communities.

DATA AVAILABILITY STATEMENT

The raw data supporting the conclusions of this manuscript will be made available by the authors, without undue reservation, to any qualified researcher.

AUTHOR CONTRIBUTIONS

XL and CC conducted the main experiments and wrote the manuscript. YiZ, MZ, and QZ carried out bioassays. JL did the ECD calculations. JW and ZL analyzed the spectroscopic data. HZ and YoZ initiated and oversaw all research. All authors reviewed the manuscript.

ACKNOWLEDGMENTS

This work was financially supported by the Program for Changjiang Scholars of Ministry of Education of the People's Republic of China (No. T2016088); the National Natural

Science Foundation for Distinguished Young Scholars (No. 81725021); Innovative Research Groups of the National Natural Science Foundation of China (81721005); the Academic Frontier Youth Team of HUST; and the Integrated Innovative Team for Major Human Diseases Program of Tongji Medical College (HUST). We thank the Analytical and Testing Center at Huazhong University of Science and Technology for assistance in the acquisition of the ECD, UV, and IR spectra.

REFERENCES

- Bourjot, M., Leyssen, P., Neyts, J., Dumontet, V., and Litaudon, M. (2014). Trigocherrierin A, a potent inhibitor of chikungunya virus replication. *Molecules* 19, 3617–3627. doi: 10.3390/molecules19033617
- Chen, K., Zhang, X., Sun, W., Liu, J., Yang, J., Chen, C., et al. (2017). Manginoids A–G: seven monoterpene–shikimate-conjugated meroterpenoids with a spiro ring system from *Guignardia mangiferae*. *Org. Lett.* 19, 5956–5959. doi: 10.1021/acs.orglett.7b02955
- Gontijo de Souza, G., Oliveira, T. S., Takahashi, J. A., Collado, I. G., Macias-Sanchez, A. J., and Hernandez-Galan, R. (2012). Biotransformation of clovane derivatives. Whole cell fungi mediated domino synthesis of *rumphellclovane A*. *Org. Biomol. Chem.* 10, 3315–3320. doi: 10.1039/C2OB07114B
- Guo, J., Tian, J., Yao, G., Zhu, H., Xue, Y., Luo, Z., et al. (2015). Three new 1 α -alkyldaphnane-type diterpenoids from the ?ower buds of *Wikstroemia chamaedaphne*. *Fitoterapia* 106, 242–246. doi: 10.1016/j.fitote.2015.09.017
- He, W., Cik, M., Appendino, G., Puyvelde, L. V., Leysen, J. E., and De Kimpe, N. (2002). Daphnane-type diterpene orthoesters and their biological activities. *Mini. Rev. Med. Chem.* 2, 185–200. doi: 10.2174/1389557024605492
- Iida, M., Ooi, T., Kito, K., Yoshida, S., Kanoh, K., Shizuri, Y., et al. (2008). Three New polyketide–terpenoid hybrids from *Penicillium* sp. *Org. Lett.* 10, 845–848. doi: 10.1021/ol7029867
- Ji, X. J., Huang, H., and Ouyang, P. K. (2011). Microbial 2,3-butanediol production: a state-of-the-art review. *Biotechnol. Adv.* 29, 351–364. doi: 10.1016/j.biotechadv.2011.01.007
- Kmiecik, N., and Zymanczyk-Duda, E. (2017). Enantio convergent biotransformation of O,O-dimethyl-4-oxoazetidin-2-ylphosphonate using fungal cells of *Penicillium minioluteum* and purified enzymes. *Bioorg. Chem.* 71, 81–85. doi: 10.1016/j.bioorg.2017.01.014
- Li, L., Knickelbein, K., Zhang, L., Wang, J., Obrinske, M., Ma, G. Z., et al. (2015). Amphiphilic sugar poly (orthoesters) as pH-responsive nanoscopic assemblies for acidity-enhanced drug delivery and cell killing. *Chem. Commun.* 51, 13078–13081. doi: 10.1039/C5CC04078G
- Liao, G. S., Chen, H. D., and Yue, J.-M. (2009). Plant orthoesters. *Chem. Rev.* 109, 1092–1140. doi: 10.1021/cr0782832
- Liu, F., Yang, X., Ma, J., Yang, Y., Xie, C., Tuerhong, M., et al. (2017). Nitric oxide inhibitory daphnane diterpenoids as potential anti-neuroinflammatory agents for AD from the twigs of *Trigonostemon thyrsoideus*. *Bioorg. Chem.* 75, 149–156. doi: 10.1016/j.bioorg.2017.09.007
- Luo, M., Cui, Z., Huang, H., Song, X., Sun, A., Dang, Y., et al. (2017). Amino acid conjugated anthraquinones from the marine-derived fungus *Penicillium* sp. SCSIO soft101. *J. Nat. Prod.* 80, 1668–1673. doi: 10.1021/acs.jnatprod.7b00269
- Meng, L. H., Wang, C. Y., Mandi, A., Li, X. M., Hu, X. Y., Kassack, M. U., et al. (2016). Three Diketopiperazine alkaloids with spirocyclic skeletons and one bithiodiketopiperazine derivative from the mangrove-derived endophytic fungus *Penicillium brocae* MA-231 *Org. Lett.* 18, 5304–5307. doi: 10.1021/acs.orglett.6b02620

SUPPLEMENTARY MATERIAL

The Supplementary Material for this article can be found online at: <https://www.frontiersin.org/articles/10.3389/fchem.2018.00605/full#supplementary-material>

The Supplementary Material includes Full NMR, HRESIMS, UV, and IR spectra of 1 and 2; detailed of the ECD calculations of 1 and 2; X-ray data of 1 and 2 (PDF); and crystallographic data (CIF).

- Ngokpol, S., Suwakulsiri, W., Sureram, S., Lirdprapamongkol, K., Aree, T., Wiyakrutta, S., et al. (2015). Drimane sesquiterpene-conjugated amino acids from a marine isolate of the fungus *Talaromyces minioluteus* (*Penicillium Minioluteum*). *Mar. Drugs* 13, 3567–3580. doi: 10.3390/md13063567
- Rank, C., Phipps, R. K., Harris, P., Fristrup, P., Larsen, T. O., and Gottfredsen, C. H. (2008). Novofumigatonin, a new orthoester meroterpenoid from *Aspergillus novofumigatus*. *Org. Lett.* 10, 401–404. doi: 10.1021/ol7026834
- Roy, A., and Saraf, S. (2006). Limonoids: overview of significant bioactive triterpenes distributed in plants kingdom. *Biol. Pharm. Bull.* 29, 191–201. doi: 10.1248/bpb.29.191
- Santana, L., Uriarte, E., Roleira, F., Milhazes, N., and Borges, F. (2004). Furocoumarins in medicinal chemistry. Synthesis, natural occurrence and biological activity. *Curr. Med. Chem.* 11, 3239–3261. doi: 10.2174/0929867043363721
- Steyn, P. S., and van Heerden, F. R. (1998). Bufadienolides of plant and animal origin. *Nat. Prod. Rep.* 15, 397–413. doi: 10.1039/A815397Y
- Sun, J., Zhu, Z. X., Song, Y. L., Dong, D., Zheng, J., Liu, T., et al. (2016). Nitric Oxide Inhibitory Meroterpenoids from the Fungus *Penicillium purpurogenum* MHZ 111. *J. Nat. Prod.* 79, 1415–1422. doi: 10.1021/acs.jnatprod.6b00160
- Tang, H. Y., Zhang, Q., Gao, Y. Q., Zhang, A. I., and Gao, J. M. (2015). Miniolins A–C, novel isomeric furanones induced by epigenetic manipulation of *Penicillium minioluteum*. *RSC Adv.* 5, 2185–2190. doi: 10.1039/C4RA11712C
- Xiao, N., Gao, J., Cai, X., and She, Z. (2009). Secondary metabolites of mangrove endophytic fungus SK5 in the South China Sea. *Zhongyaocai* 32, 1843–1845. doi: 10.3321/j.issn:1001-4454.2009.12.017
- Zhou, P., Wu, Z., Tan, D., Yang, J., Zhou, Q., Zeng, F., et al. (2017). Atrichodermones A–C, three new secondary metabolites from the solid culture of an endophytic fungal strain, *Trichoderma atroviride*. *Fitoterapia* 123, 18–22. doi: 10.1016/j.fitote.2017.09.012
- Zhu, H., Chen, C., Xue, Y., Tong, Q., Li, X. N., Chen, X., et al. (2015). *Asperchalsine A*, a cytochalasin dimer with an unprecedented decacyclic ring system, from *Aspergillus flavipes*. *Angew. Chem. Int. Ed.* 54, 13374–13378. doi: 10.1002/anie.201506264
- Zhu, H. J. (2015). *Organic Stereochemistry: Experimental and Computational Methods*. Weinheim: Wiley-VCH Verlag GmbH and Co. KGaA.

Conflict of Interest Statement: The authors declare that the research was conducted in the absence of any commercial or financial relationships that could be construed as a potential conflict of interest.

Copyright © 2018 Liu, Chen, Zheng, Zhang, Tong, Liu, Zhou, Wang, Luo, Zhu and Zhang. This is an open-access article distributed under the terms of the Creative Commons Attribution License (CC BY). The use, distribution or reproduction in other forums is permitted, provided the original author(s) and the copyright owner(s) are credited and that the original publication in this journal is cited, in accordance with accepted academic practice. No use, distribution or reproduction is permitted which does not comply with these terms.